CrossMark

ORIGINAL ARTICLE

Development of a micropump composed of three gears with Logix tooth profiles fabricated by micromilling technology

Zhenyu Shi[1,2] · Tianming Zhao[1,2] · Yi Wan[1,2] · Xianzhi Zhang[3]

Abstract Sustainability is a growing interest for industry to integrating and assessing social, environmental, and economic objectives. Involute gear and single-pump feed technology are difficult to satisfy the requirements of sustainability for high-homogeneous medium and low-loss situations. To improve the relative displacement and reduce the volume of the pump, an innovative three-gear micropump was designed. The gears were patterned with Logix tooth profiles which have lower undercutting tendency and are easy to design with a reduced number of teeth. The double-pump confluence technology was used to reduce the flow pulsation based on phase compensation. In this paper, the structural parameters of Logix gear were first calculated through mathematical analysis. Then, a micropump composed of three Logix gears was designed based on the selected parameters and double-pump confluence technology. The Logix gear was manufactured by micromilling experiments, and the three-gear pump was assembled. At last, a pressure fluctuation test platform was implemented to investigate the fluctuation of the three-gear pump and the transmission noise. Results showed that the displacement of the three-gear micropump was doubled compared with the conventional involute gear pump, with 50% flow pulsation reduction. The transmission noise of the Logix gear pump was also reduced. The outcome of this research will contribute to the development of simplified, safer and anti-fuel-burning gear pump systems, and environment-friendly and sustainable manufacturing of such systems.

1 Introduction

The environmental regulations determine that the manufacturing industry needs to take an active role in the development of clean manufacturing processes and recyclable products. The ultimate goal is the sustainable development and environmental releases for manufacturing industry. Gears and subsequently the gear manufacturing industry play an integral role in many industrial segments, as it supplies one of the basic mechanical components for transmission of motion and (/or) power to keep machines, instruments, and equipment operational [1].

Gear pump has the advantages such as simple structure, strong self-absorption ability, not sensitive to oil pollution, and easy maintenance. It is widely used in medium and low pressure hydraulic systems, lubrication systems, especially in medical, aerospace, precision instruments areas [2]. The recent developments to achieve sustainability in gear manufacturing can be summarized as material saving, waste reduction, minimizing energy consumption and maintaining economic efficiency by reducing the number of gear manufacturing stages, etc.

The traditional gear pump is difficult to adapt to the miniaturization and the demand in special applications. Hence, the design and processing of micro-gear pumps need to be further improved [3]. There are two aspects which can be improved in design of micro-gear pumps.

✉ Xianzhi Zhang
X.Zhang@kingston.ac.uk

[1] Key Laboratory of High Efficiency and Clean Mechanical Manufacture, Shandong University, Ministry of Education, Jinan, People's Republic of China

[2] School of Mechanical Engineering, Shandong University, Jinan, People's Republic of China

[3] School of Mechanical and Aerospace Engineering, Kingston University, London, UK

🖄 Springer

On the one hand, the prime issue regarding the design of micro-gear pump is to miniaturize it. The existing gear miniaturization programs generally follow the two technical ideals: reducing the modulus or reducing the number of teeth. The reduction of the modulus will decrease the bearing capacity of the gear. In the occasion of high-bearing capacity requirements, reducing the number of teeth is the only option. Usually, the gear pump has the undercut tendency which is based on the involute cylindrical gear [4]. The minimum tooth number is no less than 14–17. Even for changeable gear, the number of tooth is rarely less than 10 [5]. The traditional gear cannot meet the need of reducing the number of teeth. Logix gear is composed of many micro involutes, and every meshing point for a micro involute does not exceed the undercut boundary. By using Logix gear, the number of teeth can be greatly reduced to 3–4 [6]. Komori et al. [7] pointed that by developing a Logix tooth profile, a spur gear can have zero relative curvature at contact points under the engagement through the concave/convex pattern of contact. The Logix tooth profile can realize a spur gear whose surface durability is as high as that of the W-N tooth profile. Feng et al. [8] studied the forming principle of Logix gear tooth profile and established a theoretical model for describing the geometrical formations of this type of gear. It was found that for Logix gear, it has specific parameters such as preliminary pressure angle, relative pressure angle, and preliminary referential circle radius. Hence, reasonable selection of parameters for Logix gear is important.

On the other hand, in the occasion of high-homogeneous medium work requirements, the single-pump oil supply technology is difficult to ensure the smooth transmission of medium. The instantaneous flow for gear pump is periodic parabolic curve. By using of dual-pump converging technology, the phase difference between the two pumps can be appropriately staggered and can be compensate for each other, which in turn reduce the flow pulsation.

In recent years, with the rapid development of science and technology, ultra-precision machining technology is promising for potential applications in the fabrication field of gear pump systems. Compared with other methods, high-speed micromilling process receives much attention because of its high machining accuracy, processing efficiency, simple preparation, relatively low cost, and fewer limitations on processing materials [9, 10].

In this paper, the structural parameters of Logix gear are calculated through mathematical method. Three-gear micropump is designed based on the parameters selection and double-pump confluence technology. Further, the Logix gear is processed through micromilling experiments, and the three-gear micropump is assembled. At last, a pressure fluctuation test platform is built to investigate the fluctuation of the three-gear micropump, and the transmission noise is tested. The flow chart of this paper is shown in Fig. 1.
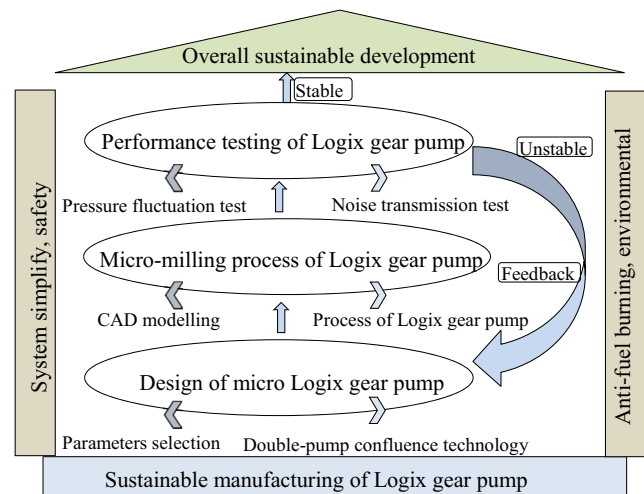

Fig. 1 Flow chart of this research

2 Double-pump confluence technology for three-gear micropump

2.1 Instantaneous flow of single pump

The instantaneous flow of single pump was investigated to study the characteristic of double-pump. Figure 2 shows the working schematic of external two-gear pump. As shown in Fig. 2, the driving gear rotates angle of $d\varphi_0$ during the time interval dt, and the driven gear rotates $d\varphi_1$ at the same time. According to the law of meshing gear, the angular velocity is inversely proportional to the radii of the gear as shown in Eq. 1.

$$d\varphi_1 = \frac{R_0}{R_1}d\varphi_0, \tag{1}$$

where R_0 is the pitch circle radius of driving gear, and R_1 is the pitch circle radius of driven gear.

The dv represented the volume of the cycloidal oil chambers is equal to the sum of the volume swept by tooth surface around by driving gear dv_0 and driven gear dv_1, as shown in Eq. 2.

$$dv = dv_0 + dv_1 \tag{2}$$

When the driving gear rotates angle of $d\varphi_0$, the volume swept by driving gear dv_0 can be expressed as the swept area multiplied the width of the teeth B [11], as shown in Eq. 3.

$$dv_0 = B\left(\frac{R_{a_0}^2 d\varphi_0}{2} - \frac{R_{c_0}^2 d\varphi_0}{2}\right) = \frac{B}{2}\left(R_{a_0}^2 - R_{c_0}^2\right)d\varphi_0, \tag{3}$$

where R_{c0} represents the radius of meshing point of driving gear.

Similarly, the dv_1 for driven gear can be expressed as shown in Eq. 4:

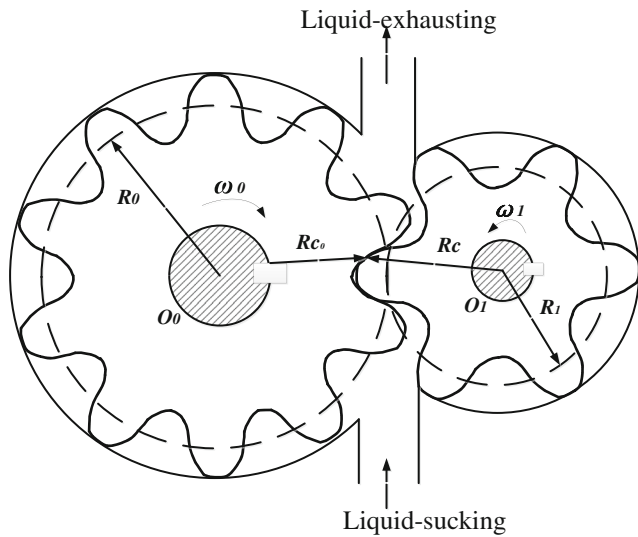$$dv_1 = \frac{B}{2}\left(R_{a_1}^2 - R_{c_1}^2\right)d\varphi_1 \tag{4}$$

Fig. 2 Working schematic diagram of external two-gear pump

The ultimate form of Eq. 2 can be written as in Eq. 5:

$$dv = dv_0 + dv_1 = \frac{B}{2}\left[\left(R_{a_0}^2 - R_{c_0}^2\right) + \left(R_{a_1}^2 - R_{c_1}^2\right)\frac{R_0}{R_1}\right]d\varphi_0 \quad (5)$$

Divided by dt on both sides in Eq. 5, the instantaneous flow of the liquid pumped from cycloidal oil chambers by gear pump can be expressed in Eq. 6:

$$Q_{\text{ins}} = \frac{dv}{dt} = \frac{B}{2}\left[\left(R_{a_0}^2 - R_{c_0}^2\right) + \left(R_{a_1}^2 - R_{c_1}^2\right)\frac{R_0}{R_1}\right]\frac{d\varphi_0}{dt}$$
$$= \frac{B\omega_0}{2}\left[\left(R_{a_0}^2 - R_{c_0}^2\right) + \left(R_{a_1}^2 - R_{c_1}^2\right)\frac{R_0}{R_1}\right] \quad (6)$$

The distance between the point of gear meshing and the node of two teeth on common normal length surfaces is defined as $R_b\varphi$. The independent variable of Rc_0 and Rc_1 in Eq. 6 was simplified according to the relationship of the trigonometric function [12]. The relationship between the instantaneous flow of the gear Q_{ins} and rotation angle of driving gear can be got as shown in Eq. 7.
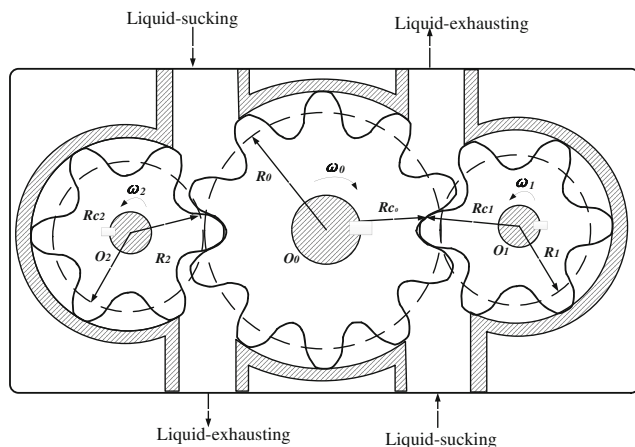

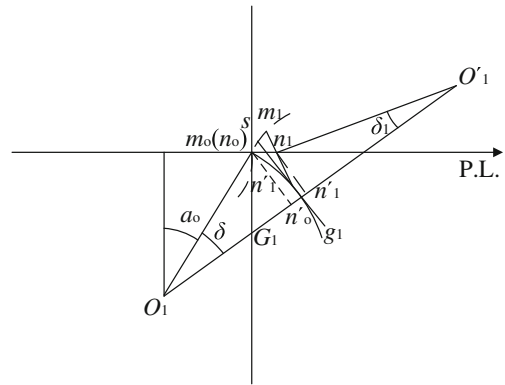Fig. 3 Working schematic for external three-gear pump

Fig. 4 Formation of involute at the initial position for Logix gear

$$Q_{\text{ins}} = \frac{B\omega_0}{2}\left[2R_0(h_0 + h_1) + h_0^2 + \frac{R_0}{R_1}h_1^2 - \left(1 + \frac{R_0}{R_1}\right)R_b^2\varphi^2\right] \quad (7)$$

2.2 Double-pump confluence technology and instantaneous flow of three-gear micropump

According to Eq. 7, the instantaneous flow of the driven gear can be expressed in Eq. 8:

$$Q_{\text{ins}}' = \frac{B'\omega_0'}{2}\left[2R_0'\left(h_0' + h_1'\right) + h_0'^2 + \frac{R_0'}{R_1'}h_1'^2 - \left(1 + \frac{R_0'}{R_1'}\right)R_b'^2\varphi'^2\right] \quad (8)$$

Hence, the instantaneous flow of dual pump converging can be expressed as following in Eq. 9:

$$Q = Q_{\text{ins}} + Q_{\text{ins}}' \quad (9)$$

As shown in Eq. 7 and Eq. 8, the instantaneous flows of dual pump converging changes with rotation angle of the gear and presented parabolic laws. The flow pulsation is decided by the phase difference of rotating angle between the two pumps. The decrease of flow pulsation can be realized through changing the phase difference between the two pumps by mutual compensation.
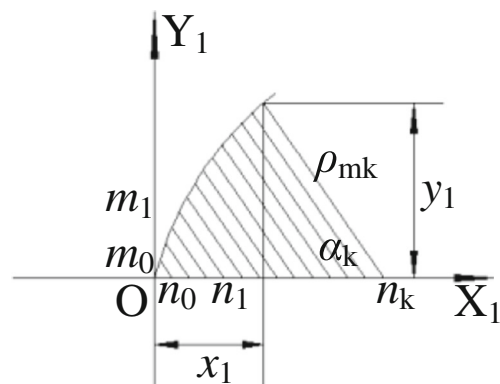

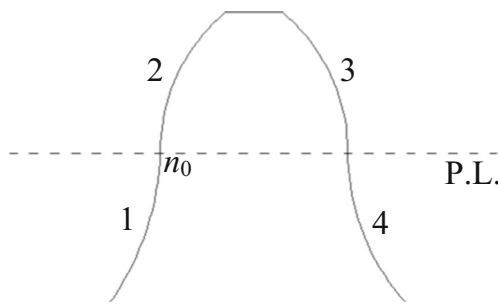Fig. 5 Coordinate sketch map of tooth profile

Fig. 6 Tooth profile section for Logix gear

Hence, in this paper, three-gear pump was adopted to realize double-pump confluence technology which can also reduce the size of the system. Figure 3 shows the working schematic for external three-gear pump.

3 Design of micro Logix gear pump

After double-pump confluence technology has been adopted, the detail of the gear can be designed. It has been investigated that [13] under the same situations, the contact fatigue strength of Logix gear is about 3 times, and the bending fatigue strength is about 2.5 times of that of involute gear. For the Logix gear, the tooth shape is formed by connecting with many micro segment involutes [14], and the principle of the tooth profile structure is similar to that of involute gear. According to gear meshing theory, the concave and convex of the formed Logix gear engage symmetrically. The relative curvature is zero for each micro involute combining point when meshing, which is also known as zero point. A large number of zero points on tooth can make the sliding coefficient of the gear very small. Hence, the existence of zero points can realize the rolling friction. The strength of the contact fatigue can also be increased.

The other prominent advantage for Logix gear is that it can realize fewer teeth gear. When the number of teeth is less than the minimum number of root, the undercutting would happen during meshing process. But for Logix gear, it is formed by

connecting with many micro segment involutes, and every segment corresponds to the minimum number of root. As long as the tooth number is greater than the biggest root number, there will be no undercutting. The minimum number of teeth is 3–4 for Logix gear, which is much less than that of involute gear 14–17. Therefore, it can realize the miniaturization of gear and can mechanize the miniaturization of gear pump.

3.1 Profile calculation for Logix gear

Figure 4 shows the formation principle of micro section of involute at the initial position for Logix gear.

In Fig. 4, α_0 is the angle between O_1n_0 and O_1n_1. δ is the pressure angle and there is $O_1O_1' = 2G_1$. n_0 and n_1 are intersection for two tangent circles with centers O_1 and O_1', radius G_1. PL is nodal line and curvature radius $\rho_{m0} = 0$.

According to the characteristic of involute, the radius of curvature for ρ_{s1} can be expressed as:

$$\rho_{s1} = G_1\delta \tag{10}$$

And there is:

$$\rho_{s1} = \rho_{m1} + G_1\delta_1 \tag{11}$$

Hence,

$$\rho_{m1} = \rho_{s1} - G_1\delta_1 = G_1(\delta - \delta_1) \tag{12}$$
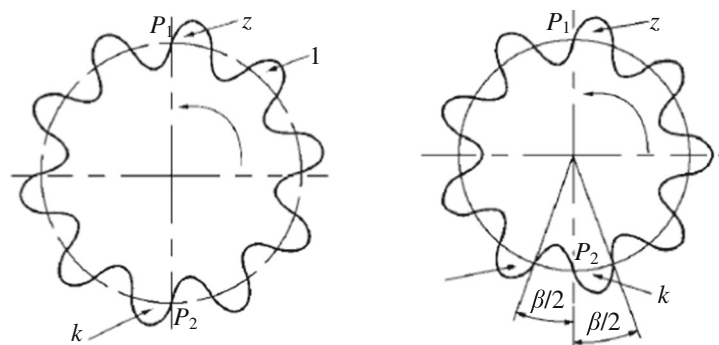$$\alpha_1 = \alpha_0 + \delta + \delta_1 \tag{13}$$

In Fig. 4, n_0n_0' and n_1n_1' are both perpendicular to O_1O_1'. n_1n_1'' is perpendicular to n_0n_0'. The angle between n_1n_0 and n_0n_1'' can be expressed in Eq. 14:

$$\angle n_1n_0n_1'' = \alpha_0 + \delta \tag{14}$$

And

$$n_1n_1'' = n_0'n_1' = O_1O_1' - O_1n_0' - O_1'n_1'$$
$$= 2G_1 - G_1\cos\delta - G_1\cos\delta_1 = G_1\cos\delta - G_1\cos\delta_1 \tag{15}$$

Fig. 7 Engaging status for driving gear

(a) Gear with even number of teeth   (b) Gear with odd number of teeth

For $\Delta\, n_0 n_1 n_1''$ is right triangle, there is:

$$\tan\angle n_1 n_0 n_1'' = \frac{n_1 n_1''}{n_0 n''} \tag{16}$$

$$\tan(\alpha_0 + \delta) = \frac{2G_1 - G_1\cos\delta - G_1\cos\delta_1}{G_1\sin\delta - G_1\sin\delta_1} = \frac{2 - (\cos\delta + \cos\delta_1)}{\sin\delta - \sin\delta_1} \tag{17}$$

δ_1 can be expressed as in Eq. 18:

$$\delta_1 = \arccos[2\cos(\alpha_0 + \delta) - \cos\alpha_0] - (\alpha_0 + \delta) \tag{18}$$

According to Eq. 12, Eq. 13, and Eq. 18, the radius curvature for one arbitrary point on tooth profile can be expressed as:

$$\rho_{mi} = \rho_{mi-1} + G_i(\delta - \delta_1) \tag{19}$$

Figure 5 shows a section of tooth profile based on the calculation.

In Fig. 5, the nodal line is set to be X_1-axis. The point of intersection n_0 between nodal line and tooth profile is set to be origin. The tooth profile in Fig. 5 can be expressed in Eq. 20:

$$\begin{cases} x_1 = n_0 n_k - \rho_{mk}\cos\alpha_k \\ y_1 = \rho_{mk}\sin\alpha_k \end{cases} \tag{20}$$

According to the formation process of tooth profile, Fig. 6 shows the other three sections of tooth profile.

From Fig. 6, it can be seen that section 1 and section 2 are in central symmetry system with n_0 as the central point. Hence, the section 1 of tooth profile in Fig. 6 can be expressed in Eq. 21:

$$\begin{cases} x_1 = -(n_0 n_k - \rho_{mk}\cos\alpha_k) \\ y_1 = -\rho_{mk}\sin\alpha_k \end{cases} \tag{21}$$

The sections 3 and 4 of tooth profile in Fig. 6 can be expressed in Eq. 22 and Eq. 23, respectively:

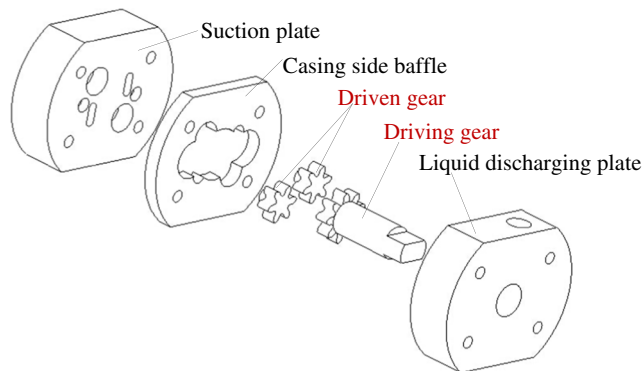$$\begin{cases} x_1 = s - (n_0 n_k - \rho_{mk}\cos\alpha_k) \\ y_1 = \rho_{mk}\sin\alpha_k \end{cases} \tag{22}$$

Fig. 8 Exploded views of structure for three-gear pump

Table 1 Parameters for Logix gear correspond to different modules

m/mm	α_0/°	δ/°	G_0/mm
1	10.0	0.050	6000
2	8.00	0.050	9500
4	6.00	0.050	10,000
5	5.00	0.050	11,000
6	4.00	0.050	12,000
8	3.20	0.050	12,024
10	2.80	0.050	14,000
12	2.60	0.050	16,500

$$\begin{cases} x_1 = s + n_0 n_k - \rho_{mk}\cos\alpha_k \\ y_1 = \rho_{mk}\sin\alpha_k \end{cases} \tag{23}$$

3.2 Selection of the number of teeth

The number of teeth for Logix gear is determined by the instantaneous flow and the characteristic of small undercut tendency. The instantaneous flow of the gear pump concerned to the meshing point of the gear. As shown in Fig. 7, the teeth of the driven gear passed are sorted clockwise from 1 to z. The intersection point of each tooth and nodal point is defined as dividing point of entry and exit of gear, which is also known as equinox of tooth profile. At the beginning of the meshing movement, the equinox of z-th tooth is coincidence with node of pitch circle P_1. The angle between z-th tooth and an arbitrary n-th tooth can be expressed as shown in Eq. 24:

$$\phi_n = 2\pi n/z \tag{24}$$

It can be seen that the instantaneous flow is decided by the engaging status of driving gear. When the driving gear had even number of teeth, there is:

$$|\pi - \phi_n| = \left|\pi - 2\pi n/2k\right| = \pi\left|1 - n/k\right|, \tag{25}$$

where $z = 2k$, k is positive integers.

According to Eq. 25, when $n = k$ and $|\pi - \phi_n| = 0$, as shown in Fig. 7a, z-th and k-th teeth rotate anticlockwise with driving
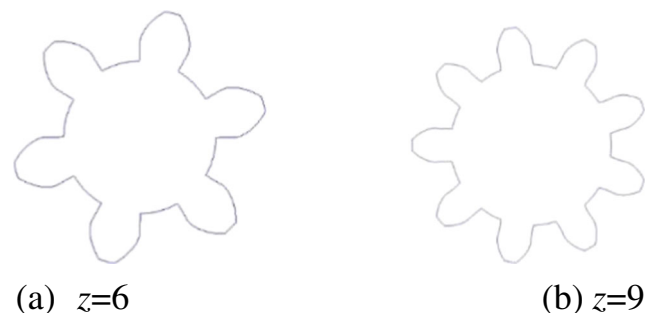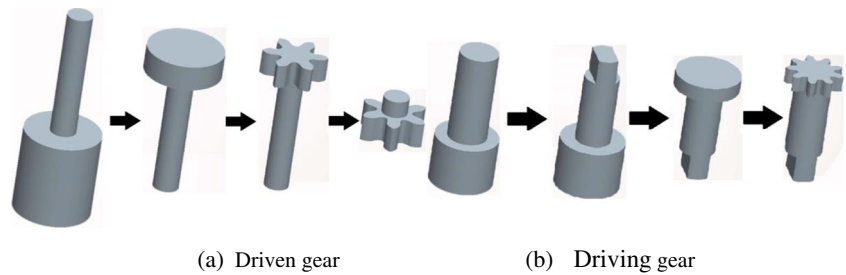

(a) $z=6$ (b) $z=9$

Fig. 9 Tooth profile of Logix gear in Pro/E

Fig. 10 The process planning of the Logix gear

(a) Driven gear   (b) Driving gear

gear. Both the two teeth profiles above nodal line are gradually engaged in meshing until disengage from the state. As shown in Fig. 7, the meshing point position for both driven gear 1 and 2 is always symmetric to driving gear. That means the phase of the instantaneous flow of two driven gears is coincident with each other.

The instantaneous flow of three-gear pump is the sum of two sub pump, which can be expressed in Eq. 26:

$$Q_{ins} = B\omega_0 \left[2R_0(h_0 + h_1) + h_0^2 + \frac{R_0}{R_1}h_1^2 - \left(1 + \frac{R_0}{R_1}\right)R_b^2\varphi_0^2 \right]$$
(26)

When the driving gear has odd number of teeth, there is $z = 2k + 1$. At the beginning of the meshing movement, the equinox of z-th tooth is coincidence with node P_1. When $|\pi - \phi_n| < \beta/2$, the profile of n-th tooth is in engaging status, which can be expressed as:

$$|\pi - \phi_n| = \left| \pi - 2\pi n/(2k + 1) \right|$$
$$= 2\pi/(2k + 1)\left| k - n + 1/2 \right| = \beta\left| k - n + 1/2 \right|$$
$$< \beta/2$$
(27)

For k and n are both positive integers, when $k \neq n$, Eq. 27 is always tenable; when $k = n$, there is $|\pi - \phi_n| = \beta|k - k + 1/2| = \beta/2$. At this time, the profile of k-th tooth is about to exist the meshing point, while the $k + 1$-th tooth is about to engage into meshing, as shown in Fig. 7b.

In Fig. 7b, it can be seen that the working section of the z-th tooth profile above the pitch line begins to engage into meshing, and the working section of the $k + 1$-th tooth profile under the pitch line begins to engage into meshing from the tooth root. There is a half tooth profile difference of the working section, when the driving gear meshed with the two driven gears.

Based on the analysis above, the instantaneous flow of the driving gear and driven gears can be expressed respectively as following:

$$Q_{ins1} = \frac{B\omega_0}{2} \left[2R_0(h_0 + h_1) + h_0^2 + \frac{R_0}{R_1}h_1^2 - \left(1 + \frac{R_0}{R_1}\right)R_b^2\varphi_0^2 \right]$$
(28)

$$Q_{ins2} = \frac{B\omega_0}{2} \left[2R_0(h_0 + h_1) + h_0^2 + \frac{R_0}{R_1}h_1^2 - \left(1 + \frac{R_0}{R_1}\right)R_b^2(\varphi_0 - \beta/2)^2 \right]$$
(29)

When $z = 2k + 1$, the overall instantaneous flow of multi-Logix-gears pump can be expressed in Eq. 16.

$$Q = \frac{B\omega_0}{2} \left\{ 4R_0(h_0 + h_1) + 2h_0^2 + 2\frac{R_0}{R_1}h_1^2 - \left(1 + \frac{R_0}{R_1}\right)R_b^2\left[\varphi_0^2 + (\varphi_0 - \beta/2)^2\right] \right\}$$
(30)

According to Eq. 26 and Eq. 30, it can be seen that when the tooth number of driving gear is even, the pulse condition is the same as the two-gear pump. When the tooth number is odd, the pulse condition is smaller than that of two-gear pump. Therefore, the tooth number of driving gear should be odd.

Table 2 Process route of Logix gear

| Gear	Procedure and dimensions	Cutting tool
Driven gear (×2)	Rough machining till length <20 mm	Cutting tool with tool shank diameter 6 mm
	Machining gear shaft	Cutting tool with tool shank diameter 6 mm
	Micromilling till gear body = 3 mm	Cutting tool with tool shank diameter 6 mm
	Micromilling of gear profile	Rough milling with the tool diameter 2 mm, finish milling with the tool diameter 1 mm
Driving gear	Rough machining till length <20 mm	Cutting tool with tool shank diameter 6 mm
	Machining gear shaft	Cutting tool with tool shank diameter 6 mm
	Micromilling till gear body = 3 mm	Cutting tool with tool shank diameter 6 mm
	Micromilling of gear profile	Rough milling with the tool diameter 2 mm, finish milling with the tool diameter 1 mm
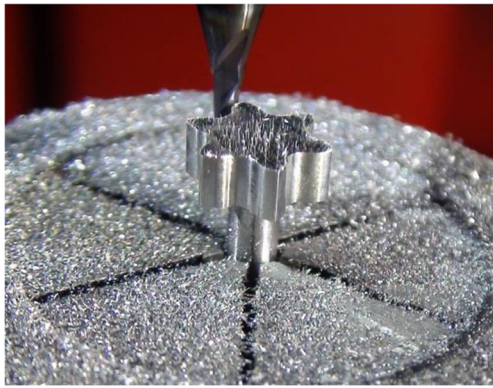
Fig. 11 Machining of driving gear

According to the analysis above, considering the limitation of gear processing equipment and materials, and the advantage of small undercut tendency of Logix gear, the tooth number of driving gear is set to be 9 (odd number), and the tooth number of the two driven gears is set to be 6.

3.3 Selection of gear module

The pump used for hydraulic lifting with displacement $q = 0.16$ ml/rev is consulted to design the gear pump in this paper. The displacement of the three-gear pump can be calculated according to Eq. 31:

$$q = 4\pi m^2 B z_0 \tag{31}$$

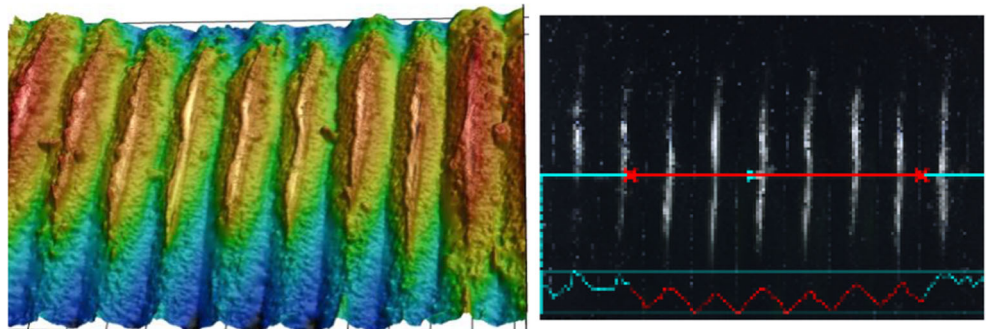The tooth width is calculated with empirical equation in Eq. 32:

$$B = (8\sim12)m \tag{32}$$

The module can be got through Eq. 33:

$$m = \sqrt[3]{\frac{q}{4\pi \times 8 \times z_0}} \approx 0.5613\text{mm} \quad (\text{where } B = 8\text{m}) \tag{33}$$

Taking into account the leakage of gear pumps and other volumetric efficiency [9], the modulus is selected to be 1 mm.

3.4 Design of structure for micropump shell

The micropump shell is designed into three parts: suction plate, liquid discharging plate, and casing side baffle. The suction and liquid discharging plate only have imbibition and drainage hole. The casing side baffle has liquid cycle circuit hole which can be used for sealing and fixing gear and for distribution of working liquid.

The design strategy used in this paper can avoid the problem of assembly accuracy and simply the processing technology.

Figure 8 shows the exploded views of structure for three-gear pump.

In Fig. 8, the suction plate is matched with axis hole of driving gear through gear groove. The axis holes of the two driven gear fit with the driving axle which is central symmetric. The suction plate, liquid discharging plate, and casing side baffle are connected through threaded connection.

4 Micromilling processing technology of Logix gear

4.1 CAD modeling of Logix gear

The tooth profile is programmed through MatLab and saved as .ibl file which can be imported into Pro/E to get the 3-D model [15].

Table 1 showed the parameters for Logix gear corresponded to different modules [16]. In the practical programming processes of gear profile, if the value of the initial pressure angle α_0 is too large, the width of the tooth would become very tiny and the tooth thickness will be reduced on addendum circle. Hence, α_0 usually is selected to be smaller than that in Table 1. When α_0 and the value of relative pressure angle δ are defined, the tooth profile would become straighter with the increase of radius of initial base circle G_0. On the contrary, it would become to be curlier with the decrease of the radius of initial base circle. Hence, the gear with lower module should have lower G_0.

As a conclusion, considering the experimental condition, the parameters for the Logix gear are defined as following: the coefficient of addendum height of the gear $h_a* = 1$, initial
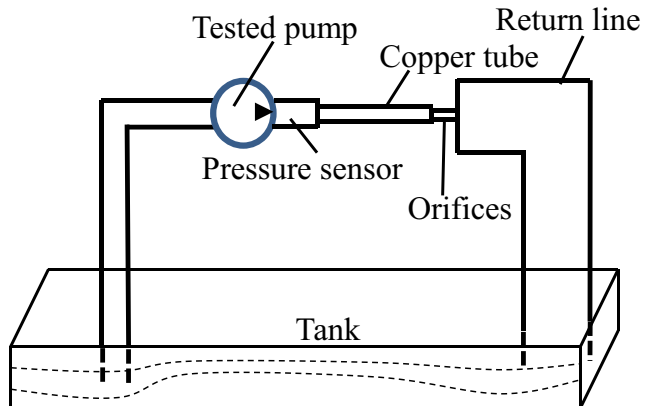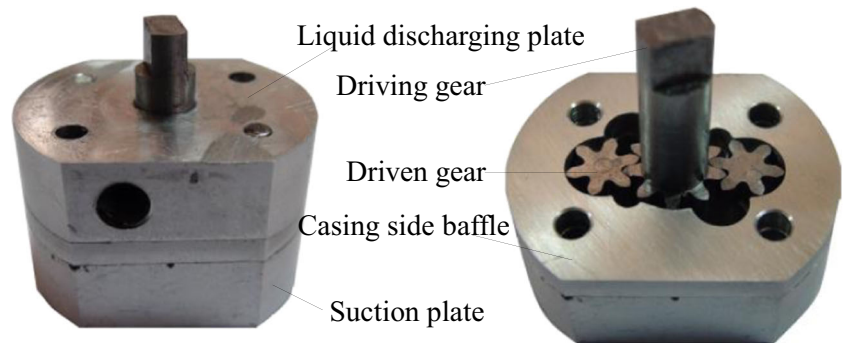
Fig. 12 Measurement surface roughness for driving gear

Fig. 13 Assembled three-gear pump

Liquid discharging plate
Driving gear
Driven gear
Casing side baffle
Suction plate

Fig. 14 Working principle of experimental station

of micromachining can reach micrometer scale, with nanometer scale surface finish. The micromachining process has become the focus of current research, since it can realize the diversification of materials, the three-dimensional structure, the complexity of the function, and the flexible automation.

In this paper, experimental work has been carried out on KERN MICRO-2522 micromilling center. Al 6061 was selected to be workpiece to reduce the manufacturing error and defects for its characteristics of good corrosion resistance, high toughness, and easy to process. Figure 10 shows the process planning of the gear. The cutting tool used was cemented carbide micromilling cutter. During micromilling process, the cutting speed was set to be 60 m/min to insurance the cutting tool life. The feed speed was selected to be 0.01 mm/r to improve the surface profile accuracy.

Table 2 showed the process route of Logix gear.

Figure 11 shows the machining process of driving gear.

The surface roughness of Logix gears is an important factor to evaluate the comprehensive quality of machined gears. In this paper, the surface roughness of the machined Logix gear was tested through an optical microscope (KEYENCE VK-X250) equipped with confocal laser scanning device.

The working surface of the gear is curved surface. During the measurement process, the measuring position is located near the pitch circle as shown in Fig. 12. The surface roughness for driving gear was obtained to be 0.79 μm and for

pressure angle $\alpha_0 = 6°$, relative pressure angle $\delta = 0.05°$, and the radius of initial base circle $G_0 = 1800$ mm.

Figure 9 shows the tool profile of Logix gear with tooth number 6 and 9 through software Pro/E.

4.2 Micromilling processing of Logix gear and assembling of gear pump

Established processing technology of micro gear includes micromachining, electrochemical machining, electrical discharge machining, embossing, and laser ablation. The precision

Fig. 15 Experimental station test for pressure fluctuation

Computer
Data acquisition board
Return line
Tank
Copper tube
Pressure sensor and orifices
Tested pump

Fig. 16 SIRIUS-S2.0 gear pump

Fig. 18 Spectral analysis of the transmission noise for conventional gear pump
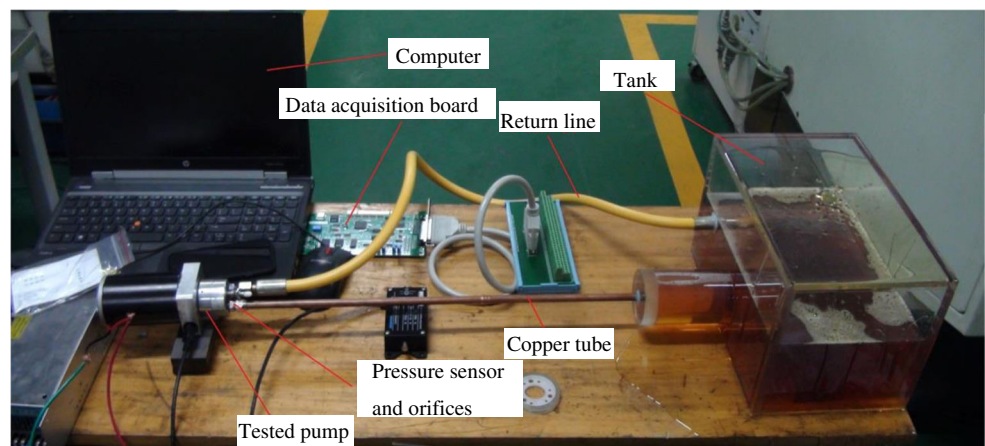
driven gear was 0.76 μm by averaging over four measurements. According to the national gear standard, the gear precision grade was 4–6.

Figure 13 shows the assembled gear pump.

5 Performance testing of processed three-gear pump

5.1 Experimental test of pressure fluctuation for micro-gear pump

A pressure fluctuation test platform was built to investigate the fluctuation of the three-gear micropump. The experimental procedure was based on the international standard ISO 10767-2. It is a method of measuring pressure pulsation for components in hydraulic system. In this paper, charge amplifier and other devices were added to analyze the pressure signals. Based on the signals collected, the pressure pulse curves can be plotted.

Figure 14 shows the working principle of the experimental station. First, the hydraulic fluid is inhaled into the tested oil pump from the tank. Then, the fluid flows past the exit of the pump through high-frequency pressure sensor, and the pressure signal can be got. The fluid then passes the copper tube, subsequently through orifices, and finally flows back to the tank.

The key technology of the test method is to produce high pressure resistance in the oil passage. It is realized by connecting an oil pipe with diameters changing in steps to the exit of the tested pump. The pressure fluctuation and the flow pulsation are in linear relationship, and the linear coefficient is equal to the pump impedance. Hence, the flow pulsation can be reflected by the pressure fluctuation of the exit.

According to the working principle mentioned above, the experimental station is established as shown in Fig. 15.

In Fig. 15, the tested pump is the three-Logix-gear pump. The pressure fluctuation of SIRIUS-S2.0 gear pump is also tested as shown in Fig. 16 which is widely used in hydraulic system for the sake of comparison. The module was 5 mm, and the number of teeth was 14.

5.2 Results and analysis

The experimental data is collected through Matlab/Simulink software acquisition. Figure 17 shows the experimental curve of pressure fluctuation when running at 1000 r/min with L-HM46# anti wear hydraulic oil.

According to Fig. 17, there are 24 pulsation periods in 0.1 s for conventional gear pump. The test pulsation period for the conventional gear pump is 4.2 ms. For the three-Logix-gear pump, there are 15 pulsation periods in 0.1 s, and the time of period is 6.7 ms.
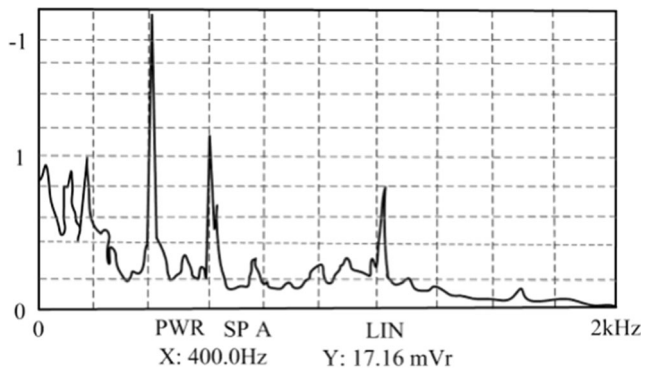
Fig. 17 Pressure fluctuation curve of two different gear pumps

Fig. 19 Spectral analysis of the transmission noise for Logix gear pump

Theoretical calculation is conducted to validate the effectiveness of the experimental results. According to the definition of flow pulsation frequency [17], the flow pulsation frequency of the conventional gear pump is calculated as shown in Eq. 34.

$$f_Q = \frac{nz}{60} = \frac{1000 \times 14}{60} = 233.3 \text{Hz} \qquad (34)$$

The pulsation period for conventional gear pump is calculated as shown in Eq. 35.

$$T = \frac{1}{f_Q} = \frac{1}{233.3} = 4.3 \text{ms} \qquad (35)$$

For Logix gear pump, the flow pulsation frequency and pulsation period are calculated as shown in Eq. 36 and Eq. 37.

$$f_Q = \frac{nz}{60} = \frac{1000 \times 9}{60} = 150 \text{Hz} \qquad (36)$$

$$T = \frac{1}{f_Q} = \frac{1}{150} = 6.7 \text{ms} \qquad (37)$$

Results show that the experiment results corresponded well with the theoretical results. For the traditional two-gear pump, the error is 2.33%, and for the Logix gear pump, the results are fully integrated.

5.3 Test of the transmission noise for the Logix gear pump

The transmission noise of gear pumps was tested on gear sound machine. Figure 18 and Figure 19 show the spectral analysis of the transmission noise for conventional gear pump and Logix gear pump.

From the results, it can be seen that the transmission noise of Logix gear pump is smaller than that of conventional gear pump. This is due to the fact that during the meshing process, the relative curvature radius is no longer zero for conventional gear with the same center distance. This leads to the decrease of contact strength and in turn increases the transmission noise for conventional gear.

6 Conclusions

A micropump composed of three gears with Logix tooth profile has been developed in this paper. The following conclusions were observed:

(1) The Logix tooth has lower undercutting tendency, and Logix gear is easy to design with a reduced number of teeth. The double-pump confluence technology can reduce the flow pulsation by phase compensation. The two technologies are efficient on reducing the volume of the micropump.

(2) A pressure fluctuation test platform was established based on the international standard ISO 10767-2. Results showed that the displacement of the designed three-gear micropump is twice of that of the two-gear pump, with 50% reduction of flow pulsation.

(3) The micromilling process was used to machine the Logix gear, and the three-gear pump was assembled. The outcome of this research will lead to system simplification and safety, anti-fuel-burning, environment-friendly, and sustainable manufacturing for micro-gear pump system.

Nomenclature

R_0	The pitch circle radius of driving gear.
R_1	The pitch circle radius of driven gear.
dv	The volume of the cycloidal oil chambers.
dv_0	The volume swept by tooth surface around by driving gear.
dv_1	The volume swept by tooth surface around by driven gear.
$d\varphi_0$	The rotate angle of driving gear.
B	The width of the teeth.
R_{c0}	The radius of meshing point of driving gear.
Q_{ins}	The instantaneous flow of the driving gear.
Q'_{ins}	The instantaneous flow of the driven gear.
Q	The instantaneous flows of dual pump converging.
δ	The pressure angle.
ρ_{s1}	The radius of curvature for involute.
q	The displacement of the three-gear pump.
m	The module of designed gear.
f_Q	The flow pulsation frequency.
T	The pulsation period.
n	The rotation speed of gear pump.
z	The number of teeth.

References

1. Jeong M, Lee S, Yoon J, Choi T (2013) Green manufacturing process for helical pinion gear using cold extrusion process. Int J Precis Eng Manuf 14:1007–1011

2. Yun J, Jeong M, Lee S, Jeon J, Park J, Kim G (2014) Sustainable production of helical pinion gears: environmental effects and product quality. Int J Precis Eng Manuf-Green Tech 1:37–41

3. Dornfeld D (2014) Moving towards green and sustainable manufacturing. Int J Precis Eng Manuf-Green Tech 1:63–66

4. Komori T, Nagata S (1988) A new gear profile of relative curvature being zero at contact points. Proceeding of International Conference on Gearing. China, CMES p 39–42

5. Feng X, Wang A, Lee L (2004) Study on the design principle of the logix gear tooth profile and the selection of its inherent basic parameters. Advan Manuf Techn 24:789–793

6. Wagner M, Ng F, Dhande S (1992) Profile synthesis and kinematic analysis of pure rolling contact gears. J Mech Design 114:326–333

7. Komori T, Ariga Y, Nagata S (1990a) A new gears profile having zero relative curvature at many contact points (LogiX tooth profile). J Mech Des 112:430–436

8. Feng X, Wang A, Lee L, Lee L (2002) Study for the forming principle of Logix gear tooth profile and its mesh performance. J Xiamen University (Nat Sci) 41:91–92

9. Wu T, Cheng K (2013) Micro milling performance assessment of diamond-like carbon coatings on a micro-end mill. Proc IMechE Part J: J Eng Trib 227:1038–1046

10. Cheng K, Huo D (2013) Micro cutting: fundamentals and applications. Wiley, Chichester

11. Yang D, Tong S, Lin J (1999) Deviation function based pitch curve modification for conjugate pair design. J Mech Design 121:579–586

12. Komori T, Alga Y, Nagata S (1990b) A new gear profile having zero relative curvature at many contact points. Trans ASME 112:430–436

13. Liu Y, Shi W, Zhang Y (2010) Analysis on qualities of bio-etching processing micro-gear part. International Conference on Mechanic Automation and Control Engineering, June 26–28, Wuhan, China

14. Horiuchi T, Furuuchi Y, Nakamura R (2006) Micro-fabrication using optical projection lithography on copper-clad plastic substrates and electroplating of nickel. Microelect Eng 83:1316–1320

15. Costopoulos T, Kanarachos A, Pantazis E (1988) Reduction of delivery fluctuation and optimum tooth profile of spur gear rotary pumps. Mecha Mach Theor 23:141–146

16. Yamasaki T (1985) Design and manufacture of noncircular gears and their applications. Mach Design 29:47

17. Gupta K, Laubscher RF, Davim J, Jain NK (2016) Recent developments in sustainable manufacturing of gears: a review. J Clea Prod 112:3320–3330